Heliyon 6 (2020) e05396

Contents lists available at ScienceDirect

Heliyon

journal homepage: www.cell.com/heliyon

Research article

Bioavailable wine pomace attenuates oxalate-induced type II epithelial mesenchymal transition and preserve the differentiated phenotype of renal MDCK cells

Gisela Gerardi [a], Cecilia I. Casali [b,c], Mónica Cavia-Saiz [a], María D. Rivero-Pérez [a], Cecilia Perazzo [b], María L. González-SanJosé [a], Pilar Muñiz [a,*,1], María C. Fernández Tome [b,c,1]

[a] Department of Food Biotechnology and Science, Faculty of Sciences, University of Burgos, Plaza Misael Bañuelos, 09001, Burgos, Spain
[b] Universidad de Buenos Aires, Facultad de Farmacia y Bioquímica, Departamento de Ciencias Biológicas, Cátedra de Biología Celular y Molecular, Buenos Aires, Argentina
[c] Universidad de Buenos Aires, Consejo Nacional de Investigaciones Cientfficas y Técnicas, Instituto de Química y Fisicoquímica Biológicas Prof. Dr. Alejandro C. Paladini (IQUIFIB)-Facultad de Farmacia y Bioquímica, Buenos Aires, Argentina

ARTICLE INFO

Keywords:
Food science
Cell biology
Plant products
Cell differentiation
Cytoskeleton
Natural product
Polyphenol
Antioxidant
Cancer research
Renal system
Wine pomace
Polyphenols
EMT
Oxalate
E-cadherin

ABSTRACT

The functional renal epithelium is composed of differentiated and polarized tubular cells with a strong actin cortex and specialized cell-cell junctions. If, under pathological conditions, these cells have to resist higher kidney osmolarity, they need to activate diverse mechanisms to survive external nephrotoxic agents such as inflammation and oxidative stress. Wine pomace polyphenols exert protective effects on renal cells. In this study, two wine-pomace products and their protective effects upon promotion and preservation of normal cell differentiation and attenuation of oxalate-induced type II epithelial mesenchymal transition (EMT) are evaluated. Treatment with gastrointestinal and colonic bioavailable fractions from red (rWPP) and white (wWPP) wine pomaces, both in the presence and the absence of oxalate, showed similar cell numbers and nuclear size than the non-treated differentiated MDCK cells. Immunofluorescence analysis showed the reduction of morphological changes and the preservation of cellular junctions for the rWPP and wWPP pre-treatment of cells exposed to oxalate injury. Hence, both rWPP and wWPP attenuated oxalate type II EMT in MDCK cells that conserved their epithelial morphology and cellular junctions through the antioxidant activities of grape pomace polyphenols.

1. Introduction

Renal medullary interstitium is characterized by its high osmolarity which plays a pivotal role in urine concentration and normal renal function. Moreover, high renal medullary interstitium osmolarity is necessary for differentiation and maturation of renal tubular structures (Pescio et al., 2017; Burg et al., 2007; Casali et al., 2013; Kültz, 2004). However, hyperosmolarity is also a stress factor that can provoke multiple alterations in cell metabolism and function. Under the conditions of an abrupt change in osmolarity, renal cells activate various osmoprotective mechanisms to adapt for survival. Osmoprotective mechanisms include the expression of diverse osmoprotective proteins, actin cytoskeleton reorganization, vimentin modification, cytokeratin expression (Casali et al., 2018; Buchmaier et al., 2013), and the metabolic upregulation of phospholipids and triglycerides (Weber et al., 2018). All these changes contribute to preserve renal structure and function. The two distinct membranes of each renal tubular cell, the basolateral membrane, immersed in interstitial tissue, and the apical membrane, in contact with urinary fluid, besides abrupt changes to their osmolarity, can expose renal cells to various pro-inflammatory stimuli such as cytokines and to toxic agents such as antibiotics, NSAIDS, metals, chemotherapeutic agents, and oxalate stones, among others (Barnett and Cummings, 2018; Getting et al., 2013). Most of them led to renal metabolic alterations, oxidative stress and fibrosis. One major characteristic of renal fibrosis is epithelial mesenchymal transition (EMT) that could be induced by several factors such as Radical Oxygen Species (ROS) and

* Corresponding author.
E-mail address: pmuniz@ubu.es (P. Muñiz).
[1] Both should be considered last author.

https://doi.org/10.1016/j.heliyon.2020.e05396
Received 16 April 2020; Received in revised form 27 September 2020; Accepted 28 October 2020

pro-inflammatory cytokines (Liu, 2010). In the EMT, renal cells lose their epithelial phenotype and acquire mesenchymal characteristics with the consequent loss of the normal epithelium function (Kanlaya et al., 2016).

Polyphenols present in wine pomaces are natural bioactive compounds with antioxidant and anti-inflammatory effects that could have protective actions against the above-mentioned types of renal damage. Holthoff et al. (2012) showed that resveratrol, a stilbene polyphenol, can protect tubular epithelial cells from peroxynitrite damage by acting as a potent scavenger of this radical. It has been demonstrated that several flavonoids inhibit EMT by interfering with TGF-β1/Smad signaling (Vargas et al., 2018). For example, epigallocatechin-3-gallate (EGCG) prevents oxalate-induced EMT in MDCK cells via induction of the Nrf2 pathway (Kanlaya et al., 2016).

In previous studies (Gerardi et al., 2019; Del Pino-García et al., 2017; Gerardi et al., 2020a; b), we have demonstrated the cytoprotective role of polyphenols found in wine pomace products against pro-oxidant and pro-inflammatory agents.

In the present work, we will evaluate two wine-pomace products and their possible effects on renal cells. On the one hand, we will determine whether wine pomace products contribute to cell differentiation and epithelial monolayer regeneration in MDCK cells growing under hyperosmolar conditions. On the other hand, we will evaluate whether wine pomace products are able to preserve functional renal cell-state differentiation and to protect renal epithelium from oxalate-induced EMT. Red and white wine pomace products digested *in vitro* were used for the evaluation of these hypotheses.

2. Materials and methods

2.1. Chemicals

2,2′-Azinobis 3-ethylbenzothiazoline-6-sulphonic acid (ABTS), porcine bile extract, (FBS), gallic acid, 6-hydroxy-2,5,7,8-tetramethyl- 2-carboxylic acid (Trolox), 2,4,6-tris(2-pyridyl)-S-triazine (TPTZ), porcine pancreas pancreatin, cellulose membrane dialysis tubing (12,000 Da molecular weight cut-off), Hoechst 33256, phalloidin-FITC conjugate, N,Obis(trimethylsilyl) trifluoroacetamide with 1% trimethylchlorosilane (BSTFA + TMS), pyridine anhydrous (99.8%), potassium persulfate, and the enzymes used in the simulated gastrointestinal digestion (α-amylase (EC 3.2.1.1), amyloglucosidase (EC 3.2.1.3), lipase (EC 3.1.1.3), and pepsin (E.C 3.4.23.1)) were obtained from Sigma-Aldrich, Co. (St. Louis, MO, USA). Ferric trichloride ($FeCl_3$), iron (II) sulfate ($FeSO_4$), sodium chloride (NaCl), potassium oxalate, paraformaldehyde, triton X-100, and sodium acetate were obtained from Panreac Química, S.L.U. (Barcelona, Spain). DMEM and Ham's F12, foetal bovine serum (FBS), antibiotic mixture, trypsin-EDTA were purchased from GIBCO®. Mouse monoclonal antibodies for β-catenin, E-cadherin, vimentin V9 and ZO-1 were obtained from Santa Cruz Biotechnology. Vectashield Mounting Medium was purchased from Vector Laboratories. Alexa Fluor® 546 Donkey anti-mouse IgG was obtained from Invitrogen-Thermo Fisher.

2.2. Wine pomace products (WPPs)

2.2.1. Wine pomace products production

Red and white wine pomace-derived products from the winemaking of *Vitis vinífera* L. cv. Tempranillo and Verdejo (rWPP and wWPP, respectively) were performed at the University of Burgos. The wine pomaces were mixed and dehydrated in an oven at 60 °C for 4 h to final moisture content <10%. Then seeds were separated from wine pomace and the remaining dried material was milled and sieved to obtain a product of particle size <0.250 nm. Heat treatment was used to obtain a stable and safe rWPP (red Wine Pomace Product) and wWPP (white Wine Pomace Product). The main characteristics and composition (dietary fiber, fat, protein, minerals, antioxidant capacity and phenolic composition) were determined previously (Gerardi et al., 2020b).

2.2.2. In vitro gastrointestinal digestion and colonic fermentation of the wine pomace products

The *in vitro* digestion of red and white wine pomace products (rWPP and wWPP) mainly involved two sequential phases that simulate conditions along the gut: enzymatic gastrointestinal digestion and colonic fermentation. Briefly, the wine pomaces (rWPP and wWPP) were incubated with pepsin (100.000 U/g, pH 2, 40 °C 1h), pancreatin (16.7 mg/g, pH 7.5, 37 °C 6h), lipase (10.000 U/g, pH 7.5, 37 °C 6h), bile salts (17 mg/g, pH 7.5, 37 °C 6h), α-amilase (8.800 U/g, pH 7, 37 °C 16h), and amyloglucosidase (10 U/g, pH 7, 37 °C 1h) and then the samples were centrifuged at 3000 g during 15 min at 25 °C. The supernatants were transferred into cellulose membrane dialysis tubing and dialyzed against Milli-Q water for 24 h. The dialysates were collected, lyophilized, weighed, and stored at -20 °C. This fraction was labelled as WPGI (Wine Pomace Gastro-Intestinal digestion). The dialysis step was performed to model the passive absorption of the intestinal barrier and obtain potentially bioavailable fractions. Then, the dialysis retentate and the residue from the centrifugation step were mixed and then subjected to an *in vitro* colonic fermentation. The microbial colonic inoculum was obtained by mixing the caecal content from 5 male Wistar rats. All procedures with these animals were performed following the guidelines established by the Ethics Committee of both the University Hospital of Burgos and the University of Burgos. The samples were incubated with the inoculum (2 g caecal content/g sample) 24 h at 37 °C in anaerobic conditions. Then, the resultant colonic fermented fractions were separated by centrifugation at 2500 g during 10 min at 25 °C. The supernatants were transferred into cellulose membrane dialysis tubing and dialyzed against Milli-Q water for 24 h. The dialysates obtained were named WPF (Wine Pomace colonic Fermentation). Three replicates were carried out for each fraction. Negative digested controls (without WPPs) for both types of fractions were also prepared.

2.2.3. Characterization of the wine pomace product-digested fractions

The *in vitro* antioxidant capacity of each fraction (rWPGI, rWPF, wWPGI and wWPF) was determined previously (Gerardi et al., 2019, 2020c) in the lyophilized powered fractions using QUENCHER (Q-) methods (Del Pino-García et al., 2015). For the QUENCHER ABTS assay (Q-ABTS), 1 ± 0.005 mg of each fraction was mixed with 10 mL of the $ABTS^{\bullet+}$ working solution (ABTS 7 mM and potassium persulfate 2,45 mM in a ratio of 1:1 (v/v)). Then, the supernatant was separated, and the absorbance was measured at 734 nm. A linear calibration curve was obtained with different amounts of Trolox as per the relevant standard. For the QUENCHER FRAP assay (Q-FRAP): 1 ± 0.005 mg of each fraction was mixed with 10 ml of the FRAP solution (10 mM TPTZ and 20 mM $FeCl_3$ in 300 mM sodium acetate buffer (pH 3.6) at a ratio of 1:1:10 (v/v/v) and diluted 10:1 (v/v) in water) and incubated at 37 ºC for 30 min with continuous stirring. Absorbance was measured at 593 nm. The results were expressed as μmol of iron (II) equivalents/g of product (Fe(II)E/g) using linear calibration obtained with different amounts of FeSO4.

The phenolic composition of each fraction was also evaluated previously by HPLC/DAD and GC/MS/MS (Gerardi et al., 2019, 2020c). Identification and quantification of stilbenes, flavan-3-ols and flavonols was carried out using analytical reversed-phase HPLC on an Agilent 1100 series HPLC system (Agilent Technologies Inc., Palo Alto, CA, USA) coupled to a diode array detector and a Spherisorb3® ODS2 reversed phase C18 column (250 mm × 4.6 mm, 3 μm particle size; Waters Cromatografia S.A., Barcelona, Spain). Samples (10 mg/ml, water solution) were injected in duplicate, and calibration was performed by injecting the standards three times at five different concentrations. Peak identification was performed by comparison of retention times and diode array spectral characteristics with the standards. The results were expressed in μg/g of digested fraction. Concentration of phenolic acids were measured in each fraction by using a gas chromatography coupled to electron ionization mass spectrometry (GC-MS/MS). 1 mg of each fraction were derivatized with 50 μL of BSTFA and 50 μL of dry pyridine, mixed and

heated at 40 ºC for 30 min. The trimethylsilyl (TMS) derivatives obtained were analyzed on an Agilent 7890B GC System (Agilent Technologies, Inc., Palo Alto, CA) coupled to an Agilent 7010 GC/MS TripleQuad detector and fitted with an DB5-MS column (25 m × 0.20 mm, 0.33 μm film thickness, Agilent Technologies) using helium as the carrier gas with an inlet pressure of 30 kPa. Injections were made in the split-less mode. For quantification, calibration curves were established by measuring peak areas versus response in comparison with the internal standard over a range of each analyte concentrations. The concentration of phenolic acids in plasma was finally expressed as μg phenolic acid/g of digested fraction.

2.3. Cell culture conditions

MDCK cells (American Type Culture Collection, passages 45–50) were seeded at a 1 × 105 cells/ml density in 6-well multidish containing glass coverslips and grown in DMEM:Ham's F12 (1:1) with 10% FBS and 1% antibiotic mixture (GIBCO®) at 37 °C in a humidified incubator with 5% CO2. After 24 h, the medium was replaced by DMEM:Ham's F12 containing 0.5% FBS to cell-cycle arrest and then, cells were incubated for another 24 h. Then, the protocols differ for the three experimental strategies:

2.3.1. Pre-differentiation assay

After 24 h incubation in DMEM:Ham's (298 ± 12 mosm/kg H_2O) containing 0.5% FBS, cells were exposed for 24 h to 2.5 μg GAE/ml of rWPGI, rWPF, wWPGI or wWPF. Then, cells were switched to a hyperosmolar medium (512 ± 12 mosm/kg H_2O) by adding aliquots of sterile 5 M NaCl to commercial medium and further incubated for 48 h. Control cells were incubated for the same periods of time but not exposed to any rWPP or wWPP digested fractions. Control isosmolar cells were incubated for the same periods of time but not exposed to NaCl or WPP fractions.

2.3.2. Post-differentiation assay

After 24 h incubation in commercial medium DMEM:Ham's F12 0.5% FBS (298 ± 12 mosm/kg H_2O), cells were switched to a hyperosmolar medium (512 ± 12mosm/kg H_2O, determined by using an osmometer (μOSMETTE, Precision Systems; Sudsbury, MA) by adding aliquots of sterile 5 M NaCl to commercial medium and further incubated for 72 h. Under these experimental conditions, epithelial monolayer is polarized and differentiated after 72 h (Pescio et al., 2012). Then, cells were exposed for 24 h to 2.5 μg GAE/ml of rWPGI, rWPF, wWPGI or wWPF. Control hyperosmolar cells were incubated for the same periods of time but not exposed to rWPP or wWPP digested fractions. Control isosmolar cells were incubated for the same periods of time but not exposed to NaCl or WPP fractions.

2.3.3. Oxalate-induced epithelial mesenchymal transition (EMT) in differentiated MDCK

It has been demonstrated that the treatment of differentiated MDCK monolayers with oxalate salts induces epithelial mesenchymal transition after 24 h (Kanlaya et al., 2016). Thus, after 24 h incubation in isosmolar conditions, cells were switched to a hyperosmolar medium (512 ± 12 mosm/kg H_2O) and further incubated for extra 72 h to reach differentiated phenotype. Then, cells were exposed to 1.5 mM potassium oxalate (oxalate-treated cells) for 24 h alone (oxalate control) or with previous treatment with to 2.5 μg GAE/ml of rWPGI, rWPF, wWPGI or wWPF. Control cells were incubated for the same periods of time but not exposed to any rWPP nor wWPP digested fractions or oxalate.

2.4. Cell number and viability

After the treatments, the cultured medium was discarded, and cells were washed twice with sterile PBS and treated with 0.25% trypsin-EDTA (GIBCO®) for 3 min. When cells were detached from the culture support, 20% of FBS was added to stop trypsin activity and cells were collected and counted in a hemocytometer chamber (Neubauer's chamber) in the presence of trypan blue to obtain the number of total and viable cells. Viability was calculated as the percentage of non-trypan blue-stained cells of total counted cells. Total viable cells were expressed as the number of trypan blue-stained cells/ml.

2.5. Fluorescence microscopy

After treatments, cells were washed twice with sterile PBS, fixed with 4% paraformaldehyde in PBS at 25 °C for 20 min and permeabilized with 0.1% Triton-X100 in PBS at 25 °C for 20 min. Fixed cells were incubated with 3% BSA in PBS at 25[a]C for 1h and further incubated for 24 h with different mouse monoclonal antibodies (Santa Cruz Biotechnology): β-catenin (1:50), E-cadherin (1:100), vimentin V9 (1:100), ZO-1 (1:50). After labeling, samples were washed with PBS and incubated with a mixture of Alexa Fluor® 546 donkey anti-mouse IgG 1:250 (Invitrogen-Thermo Fisher), phalloidin-FITC conjugate 1:50 (Sigma-Aldrich) and 2.5 μM Hoechst 33256 (Sigma-Aldrich) for 60 min. Then, samples were washed with PBS and mounted with a drop of Vectashield Mounting Medium (Vector Laboratories). Samples were examined with a Nikon Eclipse Ti microscope (with an objective Plan apo VC 60x, 1.4 DIC ½) with acquisition software Micrometric SE Premium (Accu-Scope). A minimum of 10 fields containing several cells were collected from each sample. All images were processed using Fiji ImageJ 1.52b Software (National Institutes of Health, USA).

2.6. Data presentation and statistical analysis

The results were expressed as means ± standard deviation of independent experiments (n = 3). Statistical analysis was performed using Statgraphics® Centurion XVI, version 16.2.04 (Statpoint Technologies, Inc., Warranton, VA, USA). One-way analysis of variance (ANOVA), using Fisher's least significant difference (LSD) test, was used to determine significant differences ($p < 0.05$) between data from cells incubated with the different treatments.

3. Results

In this study, MDCK cells were treated with *in vitro* digested fractions (gastrointestinal digestion and colonic fermentation) of red and white pomace products (WPGI and WPF). The objective was to evaluate the effect of the digested fractions on epithelial polarized cell phenotypes under normal conditions (NaCl-induced differentiation) and under oxalate-induced epithelial mesenchymal cell transition.

3.1. Effects of red and white pomace products on MDCK cell differentiation

MDCK cultures were pre-treated with the wine pomace fractions for 24 h and a differentiation process was then induced through incubation within a high NaCl-hyperosmolar medium for 48 h (Favale et al., 2007; Pescio et al., 2012; Casali et al., 2013), in order to evaluate whether the bioavailable gastrointestinal-digested (WPGI) and colonic-fermented (WPG) fractions of the rWPP and wWPP might affect cell differentiation. In addition, the ability of the rWPP and wWPP bioavailable fractions to preserve the integrity of the differentiated epithelium was evaluated on MDCK cells grown in a hyperosmolar medium for 72 h.

MDCK cell treatment within a high NaCl-hyperosmolar medium (Figure 1A and 1C) significantly decreased the number of cells at both 24 and 72 h. In agreement with previous studies (Burg et al., 2007; Casali et al., 2013), these results demonstrated that hyperosmolarity caused cell cycle arrest and therefore decreased cell numbers. Furthermore, hyperosmolar MDCK cells showed larger nuclear size when compared to isoosmolar cells (Figure 1B and 1D). No change to the number of cells that were collected nor in their nuclear size resulted from the addition of bioavailable WPP-digested products to MDCK cultures, pre- and

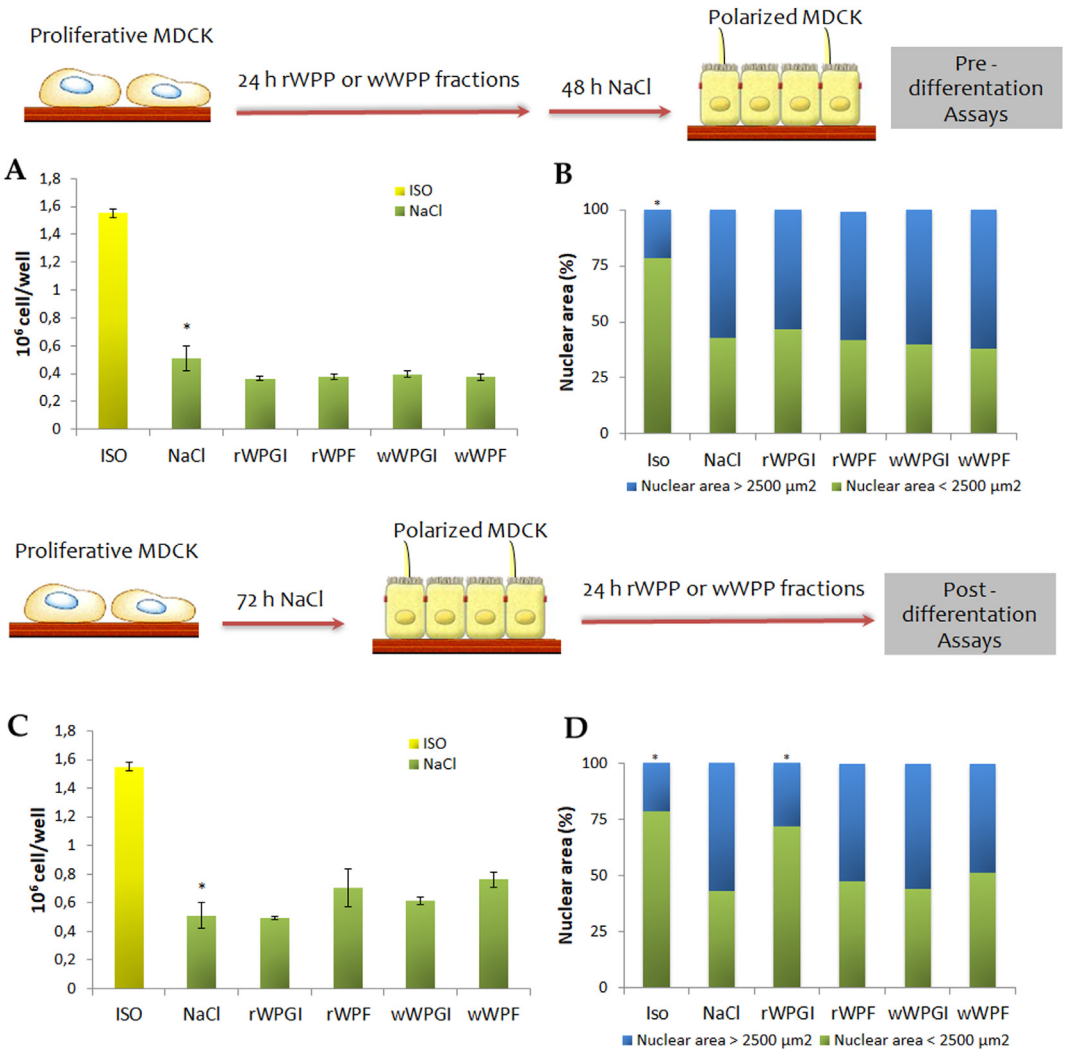

Figure 1. Cell number and nuclear size of NaCl-differentiated MDCK cells pre- and post-treated with the red and white (WPPs) digested fractions. A-B Undifferentiated MDCK cells were pre-incubated with the digested fractions of the WPPs and 24 h after were exposed to 48 h of NaCl (300 mOsm). Cell number **(A)** and nuclear area **(B)** was measurement. **C-D** Differentiated MDCK cells after 72 h exposure to NaCl (300mOsm) were post-incubated with the digested fractions of the WPPs for 24 h. Cell number **(C)** and nuclear area **(D)** was measurement. Significant differences ($p < 0.05$) between control and NaCl cells are expressed with an asterisk (*) and significant differences ($p < 0.05$) between NaCl cells and NaCl + WPPs treated cells are showed with a hash (#). ISO: MDCK cells incubated under isoosmolar conditions; NaCl: MDCK cells incubated under hyperosmolar conditions; rWPGI: MDCK cells treated with the potentially bioavailable gastrointestinal digestion fraction of the red wine pomace product; rWPF: MDCK cells treated with the potentially bioavailable colonic fermentation fraction of the red wine pomace product; wWPGI: MDCK cells treated with the potentially bioavailable gastrointestinal digestion fraction of the white wine pomace product; wWPF: MDCK cells treated with the potentially bioavailable colonic fermentation fraction of the white wine pomace product.

post-treated with hyperosmolar mediums. Therefore, the reduced proliferation and nuclear size of the differentiated cells was preserved in the presence of the WPP-digested products.

Figure 2A and 2B show the effects of the WPP-digested product on cell phenotype. Actin filaments-cytoskeleton distribution and cell morphology was assessed by fluorescence microscopy. When cells were labelled with phalloidin, anti-vimentin and anti-β-catenin (Figure 2A and 2B, a, g and m), MDCK cells cultured under isoosmolar conditions (ISO) showed a phenotype similar to an elongated fibroblast. After 48 and 72 h of hyperosmolar treatment, MDCK cell phenotype morphology assumed the typical cobblestone-like appearance, associated with a polarized-differentiated epithelial monolayer (Figure 2A and 2B, b). Vimentin stain was evident in both the isoosmolar and the hyperosmolar cells (Figure 2A and 2B, h); however, labelling appeared stronger in the isoosmolar cultures (Figure 2A and 2B, g).

Pre-treatment of isoosmolar MDCK cells with the fermented fractions of the WPPs (rWPF and wWPF) and incubation in a hyperosmolar-medium for 48 h had no effect on the cobblestone-like morphology of cells within the hyperosmolar cell cultures (Figure 2A, d and f). However, pre-treatment with the gastrointestinal fractions (rWPGI and wWPGI) induced morphological changes and increased actin stress fibers, as was observed with phalloidin staining (Figure 2A, c and e). The effect of the different digested fractions on MDCK differentiation was evaluated by analyzing their effect on actin filament cytoskeletons using phalloidin staining. The results indicated that, under isoosmolar conditions, the WPPs digested fractions induced no MDCK differentiation (Figure 3). In addition, these results suggested that gastrointestinal digested fractions (rWPGI and wWPGI) may delay differentiation processes triggered by hyperosmolarity.

The treatment of hyperosmolar MDCK cells with the digested fractions of rWPP and wWPP showed no change in the cobblestone-like morphology (Figure 2B, c, d, e and f). Instead, in the treated cells, vimentin fiber distribution assumed a discontinuous network with an increase in speck-like structures (Figure 2B, i-l). Moreover, all the cells

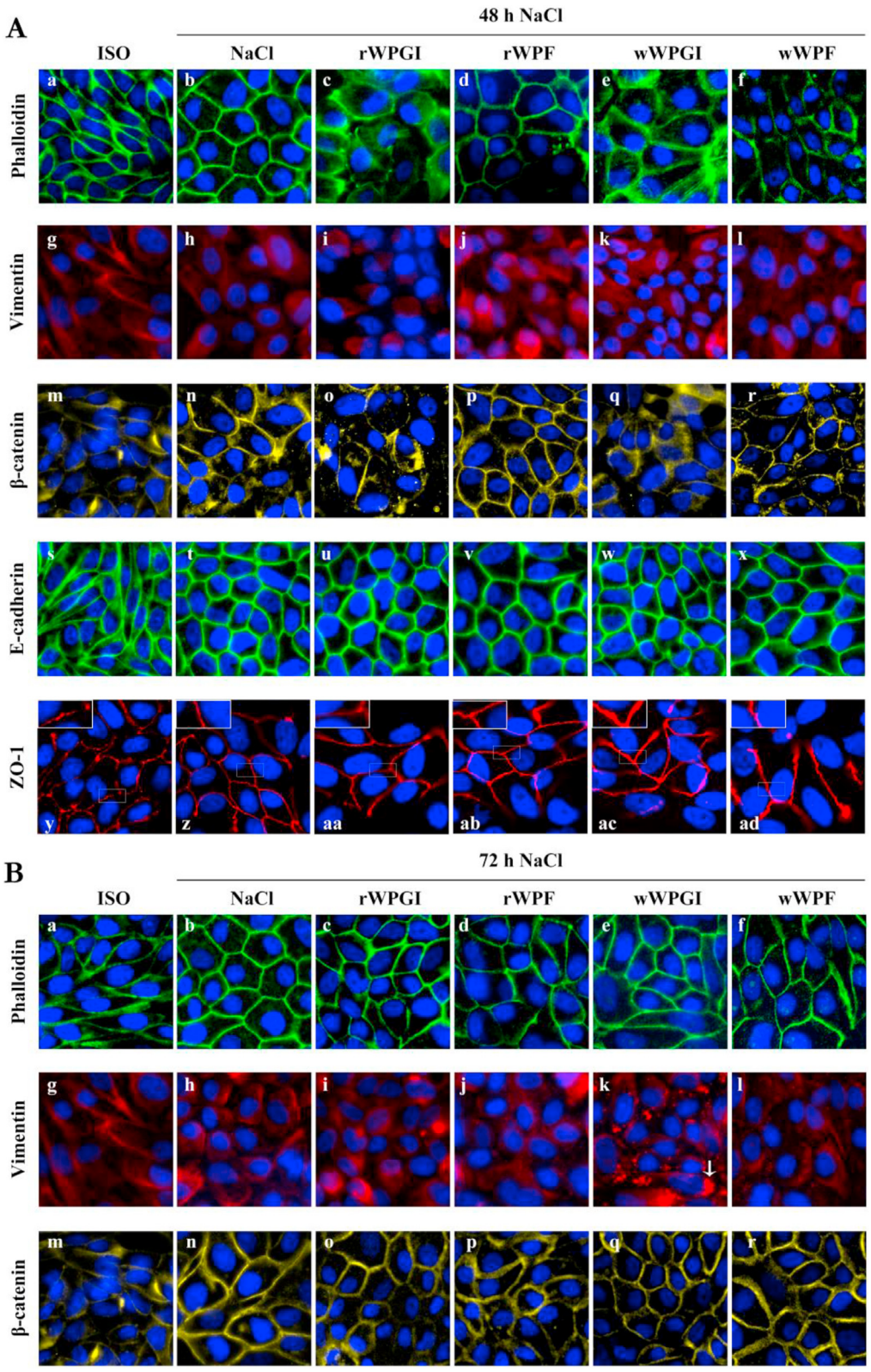

Figure 2. Cell morphology and cellular junctions of NaCl-differentiated MDCK cells treated with the red and white WPPs-digested fractions assessed by immunofluorescence. **(A)** Undifferentiated MDCK cells were pre-incubated with the digested fractions and then exposed to NaCl (300 mOsm). **(B)** Differentiated MDCK cells by NaCl (300mOsm) were post-incubated with the digested fractions. Actin filaments were assessed by phalloidin-FITC staining (a-f, green). Vimentin (g-l, red), β-catenin (m-r, yellow), E-cadherin (s-x, green) and Zonula occludens-1 (ZO-1, red, y-ad) was assessed using monoclonal antibodies. Hoechst was used for the nuclear staining (blue). ISO: cells under isoosmolarity; NaCl: cells under hyperosmolar; rWPGI, rWPF, wWPGI and wWPF: cells treated with the rWPGI, rWPF, wWPGI and wWPF (respectively).

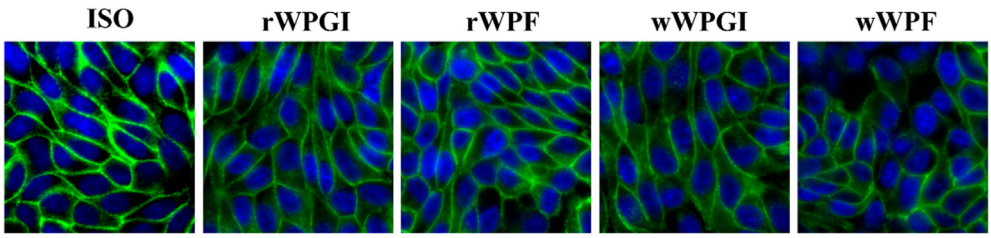

Figure 3. Phalloidin staining for MDCK cells under isoosmolar conditions non-treated with the WPPs digested fractions (ISO) and treated with the rWPGI, rWPF, wWPGI or wWPG digested fractions.

treated with the digested fractions showed vimentin labelling with perinuclear distribution, which was more marked in cells treated with the wWPGI (Figure 2B k, arrowhead).

In addition, we evaluated cell-cell junction establishment and maintenance, typical of polarized epithelia. Adherens (E-cadherin and β-catenin) and tight (ZO-1) junction proteins were analyzed by immunofluorescence (Figure 2A, m-ad, and 2B, m-r). Both E-cadherin (Figure 2A, s) and β-catenin (Figure 2A and 2B, m) were present in isoosmolar MDCK cells and cell-cell adhesions, but the typical fibroblast-like phenotype was observed. When the cells were subjected to hyperosmolar treatment for 48 h, both adherent proteins delineated the typical cobblestone-like phenotype of the differentiated epithelial MDCK

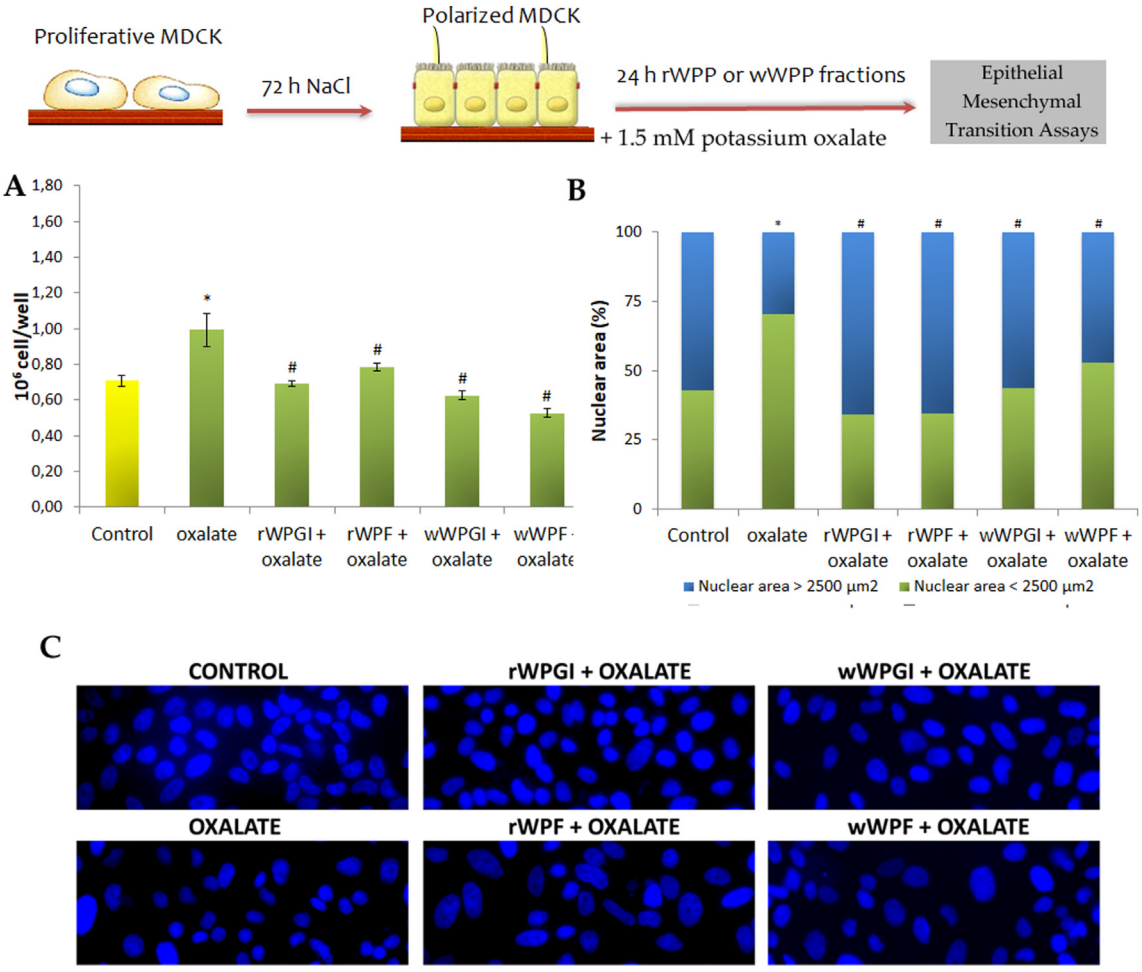

Figure 4. Cell number and nuclear size of oxalate-induced epithelial mesenchymal transition (EMT) of NaCl-differentiated MDCK cells treated with the red and white WPPs digested fractions. Differentiated MDCK cells after 72 h exposure to NaCl (300mOsm) were incubated with the digested fractions of the WPPs and with 1.5 mM of oxalate for 24 h. Cell number **(A)** and nuclear area **(B)** were measured. **(C)** Hoechst staining showing cell nuclei (blue). Significant differences ($p < 0.05$) between control and oxalate cells are expressed with an asterisk (*) and significant differences ($p < 0.05$) between oxalate cells and oxalate + WPPs treatment cells are showed with a hash (#). CONTROL: MDCK cells incubated under hyperosmolar conditions; Oxalate: MDCK cells incubated under hyperosmolar conditions and exposed to 1.5 mM of oxalate for 24 h; rWPGI: MDCK cells incubated under hyperosmolar conditions treated with the potentially bioavailable gastrointestinal digestion fraction of the red wine pomace product and exposed to 1.5 mM of oxalate for 24 h; rWPF: MDCK cells incubated under hyperosmolar conditions treated with the potentially bioavailable colonic fermentation fraction of the red wine pomace product and exposed to 1.5 mM of oxalate for 24 h; wWPGI: MDCK cells incubated under hyperosmolar conditions treated with the potentially bioavailable gastrointestinal digestion fraction of the white wine pomace product and exposed to 1.5 mM of oxalate for 24 h; wWPF: MDCK cells incubated under hyperosmolar conditions treated with the potentially bioavailable colonic fermentation fraction of the white wine pomace product and exposed to 1.5 mM of oxalate for 24 h.

monolayer (Figure 2A, n, t). Similar results were observed after 72 h of hyperosmolar treatment for β-catenin immunofluorescence (Figure 2B, n).

After 48 h of hyperosmolar treatment the distribution of E-cadherin was conserved in cells pre-treated with all the digested fractions of the rWPP and wWPP (Figure 2A, u-x). In contrast, β-catenin conserved a continuous peripheral distribution in rWPF and wWPF pre-treated cells (Figure 2A, p, r); however, when pretreated with gastrointestinal digested fractions (rWPGI and wWPGI), the β-catenin signal of the cells was reduced (Figure 2A, o, q).

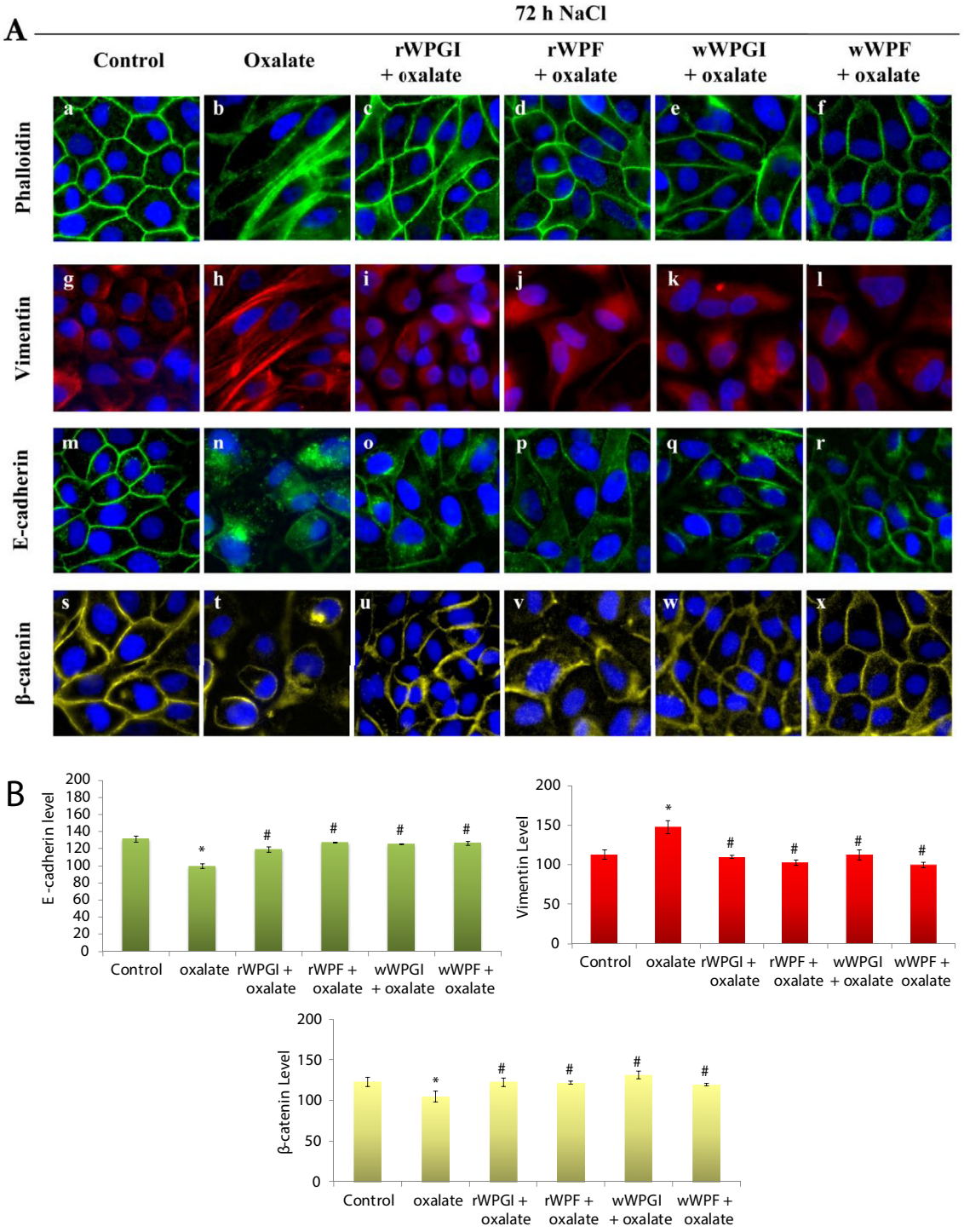

Figure 5. Cell morphology and cellular junctions of oxalate-induced epithelial mesenchymal transition (EMT) of NaCl-differentiated MDCK cells treated with the red and white WPPs digested fractions assessed by immunofluorescence. Differentiated MDCK cells after 72 h exposure to NaCl (300mOsm) were incubated with the WPP-digested fractions and 1.5 mM of oxalate for 24 h. **(A)** Phalloidin-FITC staining of actin (a-f, green). Vimentin (g-l, red), E-cadherin (m-r, green) and β-catenin (s-x, yellow) was assessed using monoclonal antibodies. Hoechst was used for the nuclear staining (blue). **(B)** E-cadherin, β-catenin and vimentin fluorescence intensity levels were assessed using Fiji ImageJ 1.52b Software. Significant differences ($p < 0.05$) between control and oxalate cells are expressed with an asterisk (*) and significant differences ($p < 0.05$) between oxalate cells and oxalate + WPPs treatment cells are showed with a hash (#). CONTROL: hyperosmolar MDCK cells; Oxalate: hyperosmolar MDCK cells exposed to oxalate; rWPGI: hyperosmolar MDCK cells exposed to rWPGI and oxalate; rWPF: hyperosmolar MDCK cells exposed to rWPF and oxalate; wWPGI: hyperosmolar MDCK cells exposed to wWPGI and oxalate; wWPF: hyperosmolar MDCK cells exposed to wWPF and oxalate.

When the cells were subjected to hyperosmolar treatments for 72 h prior to treatment with the digested fractions, the peripheral distribution of E-cadherin was conserved in all cases (Figure 2B, o-r). Thus, hyperosmolarity was seen to induce differentiation activation mechanisms that prevented the effect of digested fractions.

The tight junction protein ZO-1 showed a discontinuous peripheral distribution with a dot-like appearance in undifferentiated MDCK cells (Figure 2A, y). When the cells were exposed to 48 h of hyperosmolar treatment, the ZO-1 signal acquired a more continuous peripheral distribution (Figure 2A, z); similar features were also observed following pre-treatment with all rWPP and wWPP digested fractions (Figure 2A, aa-ad).

3.2. Red and white pomace products effect on epithelial mesenchymal transition pZhenotype (EMT) induced by oxalate

Differentiated MDCK cells (72 h NaCl) were pre-treated with 2.5 μg GAE/ml for 4 h prior to potassium oxalate treatment (1.5 mM), in order to evaluate the potential protective effect of the rWPP and wWPP-digested fractions against oxalate-induced epithelial mesenchymal transition (EMT).

After 24 h of oxalate treatment, the number of MDCK cells collected from cultures was 40 % higher compared to non-oxalate control (Figure 4A). Pre-treatment with in vitro digested fractions (gastrointestinal digestion and colonic fermentation) of red and white pomace products (WPGI and WPF) significantly reduced cell numbers, showing similar values to non-oxalate control cells (Figure 4A). Moreover, oxalate treatment significantly reduced cell nuclear size (65% with respect to the control sample), which the pre-treatment with digested fractions prevented (Figure 4B and 4C).

The typical cobblestone-like morphology found in differentiated MDCK cells was observed in untreated control samples (Figure 5A, a). After oxalate treatment, cell enlargement was observed with elongated fibroblast-like cells and visible stress fibers (Figure 5A, **b**). Pre-treatment of differentiated MDCK cultures with the gastrointestinal and colonic fermented fractions of both rWPP and wWPP prevented the establishment of oxalate-treated phenotype such as those observed in the cobblestone-like morphologies that resembled untreated control cells (Figure 5A a, c-f).

The effect of WPP treatment was evaluated for epithelial (E-cadherin and β-catenin) and mesenchymal (vimentin) phenotypes markers. Oxalate treatment significantly increased vimentin fibers (Figure 5A, h) and vimentin levels (Figure 5B) with respect to untreated control samples (Figure 5A, g and 5B). In contrast, oxalate treatment significantly decreased E-cadherin and β-catenin levels (Figure 5A, n, t and 5B). Pre-treatment with the digested fractions of both rWPP and wWPP, preserved the epithelial and mesenchymal markers at the control levels (Figure 5B). Immunofluorescence images showed that rWPP and wWPP pre-treatment partially restored vimentin (Figure 5A, i-l), E-cadherin (Figure 5A, o-r) and β-catenin (Figure 5A, u-x) to former control levels.

4. Discussion

Renal tubular structures were constituted within a typical polarized epithelium membrane transporting water and electrolyte, in order to achieve physiological functions. An MDCK (Madin-Darby canine kidney) cell line, derived from distal tubule cells or cortical collecting duct, displays the typical morphological properties of transporting epithelial cells and the formation of monolayers of highly polarized cells with apical microvilli, apical junctional complexes, desmosomes, and basolateral infoldings (Herzlinger et al., 1982; Rindler et al., 1979). The model has since been widely used for studying renal epithelial structure and functions.

Previous studies (Favale et al., 2007; Pescio et al. 2012, 2017; Casali et al., 2013) have demonstrated that MDCK cultures subjected to high NaCl-hyperosmolar medium accelerate their polarization-differentiation process. Thus, after 48–72 h of hyperosmolar treatment cells undergo morphological changes from a fibroblast-like phenotype into a polarized epithelial phenotype that includes primary cilium formation on apical membranes almost reminiscent of medullary collecting duct cells. The first morphological change observed in these cells is cytoskeleton modifications with the substitution of vimentin fibers by cortical actin filaments (Lamouille et al., 2014) as was observed in MDCK cells pre- and post-treated with the rWPP and wWPP fractions. This observation clearly indicates that wine pomace products affected neither normal differentiation nor the maintenance of renal epithelial differentiation. The establishment of cell-cell junctions is a requirement for developing polarized phenotypes, and their preservation is essential for tissue integrity. In vertebrates, cell–cell junctions can be classified into four functional classes: adherens junctions and desmosomes, which mechanically link cells by bridging the cytoskeleton of adjacent cells, communicating junctions, or gap junctions, which chemically and electrically couple neighboring cells, and occluding junctions, or tight junctions, which are essential for establishing barrier functions across a cell layer (Wei and Huang, 2013). In adherens Junction (AJ) complexes, the extracellular domain of the transmembrane protein E-cadherin interacts with cadherins within neighboring cells and the intracellular tail provides the scaffold for the armadillo family members (such as β-catenin, plakoglobin/β-catenin, and p120-catenin), which bind the cadherin tails and anchor cytoskeletal adapter proteins (such as β-catenin), which in turn anchor the AJ to the cytoskeleton and improve the stability of the AJ (Santacreu et al., 2019). Beta-catenin and E-cadherin localize in the periphery of the cells delineating cell morphology, both under isoosmolarity and hyperosmolarity as we saw for the pre- and post-treated cells with the rWPP and wWPP. However, the AJs are immature under isotonocity and become stable in hyperosmolarity-induced cell differentiation acquiring the typical cobblestone-like morphology as shown by Favale et al. (2015).

Pre-treatment of non-differentiated MDCK cells with fermented fractions of rWPP and wWPP improves the maturation of the AJ, as was seen with β-catenin staining. In contrast, β-catenin was strongly preserved in the cellular periphery when the differentiated MDCK cells were post-treated with all the WPPs fractions. However, this effect was not observed within the WPGI fractions, possibly due to their different polyphenolic compositions. The higher content of flavan-3-ols such as epigallocatechin and proantocyanidin B1 could be involved in the effect of fermented fractions (WPFs).

On the other hand, tight junctions (TJ) are responsible for regulating paracellular permeability and maintaining cell polarity (Bazzoni and Dejana, 2004). Zonula occludens-1 (ZO-1) is a main component of the TJ and increases their localization in the membrane when the cell is polarized. Pre-treatment of non-differentiated MDCK cells with the digested fractions of rWPP and wWPP conserve the ZO-1 localization during the cell differentiation contributing to the preservation of the cell polarity.

Different studies have revealed the role of polyphenols in the induction of multiple actions in the cell cycle. Hsu et al. (2003) showed that epigallocatechin gallato (EGCG), one of the major components of the rWPF and wWPF fractions, is involved in the induction of differential effects on tumor and normal cells. They found growth arrest and induction of cell differentiation in undifferentiated growing keratinocytes by EGCG while their reentry in the cell cycle in aged and differentiated keratinocytes increased their proliferation. Interestingly, our results showed that both fermented fractions of rWPP and wWPP improved the cell differentiation in non-differentiated MDCK cells, and all digested fractions, WPGI and WPF, both of rWPP and wWPP conserved the differentiated state in the MDCK epithelium without increasing cell proliferation. In this aspect, the promotion of cell differentiation and the preservation of the differentiation state have two important implications: (I) bioavailable fractions of rWPF and wWPF may contribute to kidney cell regeneration since no cytotoxic effect nor cell differentiation inhibition were observed; (II) polyphenols contained in gastrointestinal and

colonic fermented fractions of rWPP and wWPP promoted no proliferation and tumorigenesis of MDCK cultures, thus preserving cell differentiation.

During their embryonic phase, renal cells undergo a type I epithelial mesenchymal transition (EMT) and they are modified and rearranged to form the renal tubular structure (Burns and Thomas, 2010; Kalluri and a Weinberg, 2009). However, there are pathogenic EMTs that include inflammatory processes, fibrosis (type II) and cancer progression (type III). Fibrosis comprises type II EMT in which cells acquire fibroblast-like phenotype with the loss of normal epithelial functions. Cell changes during type III EMT, such as fewer cell-cell junctions and the development of vimentin cytoskeletons led to a migratory phenotype and promoted cancer metastasis (Kalluri and a Weinberg, 2009). A model of type II EMT in differentiated MDCK cells were used in this study, in order to evaluate the preventive action of the wine pomace products in this pathologic state. Previous studies (Kanlaya et al., 2016; Convento et al., 2019) showed that oxalate can induce EMT in tubular epithelial cells and thus contribute to the development of renal fibrosis (Convento et al., 2017). Convento et al. (2019) observed morphological changes in the inner medullary collecting duct (IMCD) cells consequent to oxalate treatment with downregulation of E-cadherin and formation of vimentin fibers. Our results agree with these previous reports, in so far as MDCK-differentiated monolayers treated with oxalate for 24 h changed cell morphology from cobblestone-like phenotypes to elongated fibroblast-types, developed a laxer cytoskeleton of vimentin fibers and moved E-cadherin from cell periphery to cytoplasm. It has been reported that oxalate can induce type II EMT by increasing reactive oxygen species (ROS) that act as secondary messenger to mediate type II EMT (Convento et al., 2019; Rashed et al., 2004). In previous studies (Gerardi et al., 2019, 2020a; Del Pino-García et al., 2016, 2017), we demonstrated the *in vitro* and *in vivo* antioxidant activity of wine pomaces products by acting as direct scavengers of ROS, promoting the antioxidant systems and modulating signaling pathways of the redox cellular state such as Nrf2, NF-κB and SIRT1. Thus, the capacity of bioavailable WPPs fractions to reduce ROS levels and to modulate the Nrf2/NfkB pathway may explain the protective effect exerted by rWPP and wWPP fractions on oxalate-induced EMT (Khand et al., 2002); differentiated MDCK cells therefore preserved epithelial morphology, peripheric E-cadherin and reduced vimentin fibers. This effect was observed with other antioxidants such as N-acetylcysteine (NAC) that attenuated the adverse effects of oxalate and partially inhibited oxalate-induced EMT. The observed NAC effect and the prevention of the oxalate-induced EMT by the WPPs suggests that mediators other than ROS are also involved in this transition. Moreover, WPP polyphenols such as flavonoids, proanthocyanins and catechin are known to suppress EMT and to reduce renal fibrosis (Kanlaya et al., 2016; Vargas et al., 2018).

It is also known that cytoskeleton rearrangements in EMT comprise two main events: (I) stimulation of Rac/PAK/MLC and Rac/WASP/ARP pathways, causing lamellipodia formation and cell motility and, (II) stimulation of RhoA/ROCK that increase actin stress fibers (Lamouille et al., 2014). Previous studies indicated that polyphenols of WPP such as EGCG, kaempferol, and resveratrol downregulate RhoA and Rac in several cellular systems (Kim et al., 2017; Li et al., 2017; Gray et al., 2014). Thus, the content of these compounds in the WPPs could contribute to the absence of cytoskeleton rearrangements through the modulation of RhoA and Rac signaling pathways. However, further studies are needed to evaluate the mechanism of action of WPPs on cytoskeleton rearrangements.

As mentioned above, oxalate-induced type II EMT includes a reduction of the epithelial marker E-cadherin. This alteration was observed in differentiated-MDCK cells treated with oxalate and the pretreatment with WPPs fractions exerted a cytoprotective effect on AJ, blocking the disruptive effects of cell-cell junctions possibly modulating the oxidative stress (Rao, 2008). Additionally, other changes in the protein junctions have been observed during EMT such as the redistribution of β-catenin (Lamouille et al., 2014). When β-catenin is released from the AJ, it can translocate to the nucleus and stimulate the expression of proteins associated with cell proliferation and apoptosis reduction. Curiously, the results of our study suggested that the treatment of MDCK cells with oxalate did in fact induce cell proliferation mediated by β-catenin, shown by the observed increase in cell numbers accompanied by less β-catenin staining in the cellular periphery. In contrast, an absence of cell proliferation takes place in oxalate-treated MDCK cells pre-treated with rWPP and wWPP bioavailable fractions by preventing an increase in cell numbers and maintaining β-catenin in the AJ. A possible explanation for this observation is the modulatory effect of polyphenols on Wnt pathway activation, which is required for β-catenin transcriptional activity activation (Bazzoni and Dejana, 2004; Sferrazza et al., 2020). Under normal conditions, free β-catenin is phosphorylated and degraded however this phosphorylation can be inhibited by Wnt pathway activation (Bazzoni and Dejana, 2004). Interestingly, resveratrol, quercetin, epigallocatechin and other flavonoids present in the WPPs, suppress Wnt/β-catenin pathways and could contribute to the prevention of the EMT effects in the β-catenin distribution (Dai et al., 2018; Mohana et al., 2018; Chen et al., 2017).

In summary, the rWPP and wWPP fractions conserved the differentiated and functional phenotype of the MDCK cells under normal conditions and prevented oxalate-induced type II EMT.

5. Concluding remarks

The bioavailability of phenolic compounds within red and white wine pomace products could improve renal tissue regeneration and prevent renal fibrosis by preserving differentiated epithelial phenotypes under normal and pathological conditions, as well as epithelial mesenchymal cell transition. In addition, pre-treatment with the rWPP and wWPP prior to oxalate induction prevented oxalate type II EMT in MDCK cells and conserved the epithelial morphology and cellular junctions through the antioxidant activities of their polyphenols.

Declarations

Author contribution statement

G. Geradi: Conceived and designed the experiments; Performed the experiments; Analyzed and interpreted the data; Wrote the paper.

P. Muñiz and M. del Carmen Fernández-Tome: Conceived and designed the experiments; Analyzed and interpreted the data; Contributed reagents, materials, analysis tools or data; Wrote the paper.

C. Casali, C. Perazzo and M. Rivero-Pérez: Performed the experiments.

M. Cavia-Saiz: Analyzed and interpreted the data; Wrote the paper.

M. González-SanJosé: Contributed reagents, materials, analysis tools or data; Wrote the paper.

Funding statement

This work was supported by Agencia Nacional de Promoción Científica y Tecnológica (PICT 2016-1055), the University of Buenos Aires (UBACYT 2014-2017, 20020130100658BA) and the Ministerio de Ciencia, Innovación y Universidades (PGC2018-097113B100).

Declaration of interests statement

The authors declare no conflict of interest.

Additional information

No additional information is available for this paper.

References

Barnett, L.M.A., Cummings, B.S., 2018. Nephrotoxicity and renal pathophysiology: a contemporary perspective. Toxicol. Sci. 164, 379–390.

Bazzoni, G., Dejana, E., 2004. Endothelial cell-to-cell Junctions : molecular organization and role in vascular homeostasis. Phytochem. Rev. 84, 869–901.

Buchmaier, B.S., sBibi, A., Müller, G.A., Dihazi, G.H., Eltoweissy, M., Kruegel, J., Dihazi, H., 2013. Renal cells express different forms of Vimentin : the independent expression alteration of these forms is important in cell resistance to osmotic stress and apoptosis. PLoS One 8, 1–13.

Burg, M.B., Ferraris, J.D., Dmitrieva, N.I., 2007. Cellular response to hyperosmotic stresses. Physiol. Rev. 87, 1441–1474.

Burns, W.C., Thomas, M.C., 2010. The molecular mediators of type 2 epithelial to mesenchymal transition (EMT) and their role in renal pathophysiology. Expert Rev. Mol. Med. 12, 1–18.

Casali, C.I., Erjavec, L.C., Fernández-Tome, M. del C., 2018. Sequential and Synchronized Activation of Rel-Family Transcription Factors Is Required for Osmoprotection in Renal Cells, p. 2.

Casali, C.I., Weber, K., Favale, N.O., Fernández-Tome, M.C., 2013. Environmental hyperosmolality regulates phospholipid biosynthesis in the renal epithelial cell line MDCK, 54, 677–691.

Chen, Y., Wang, X.Q., Zhang, Q., Zhu, J.Y., Li, Y., Xie, C.F., Li, X.T., Wu, J.S., Geng, S.S., Zhong, C.Y., Han, H.Y., 2017. (-)-Epigallocatechin-3-gallate inhibits colorectal cancer stem cells by suppressing Wnt/β-catenin pathway. Nutrients 9, 1–11.

Convento, M., Pessoa, E., Aragão, A., Schor, N., Borges, F., 2019. Oxalate induces type II epithelial to mesenchymal transition (EMT) in inner medullary collecting duct cells (IMCD) *in vitro* and stimulate the expression of osteogenic and fibrotic markers in kidney medulla *in vivo*. Oncotarget 10, 1102–1118.

Convento, M.B., Pessoa, E.A., Cruz, E., Da Glória, M.A., Schor, N., Borges, F.T., 2017. Calcium oxalate crystals and oxalate induce an epithelial-to-mesenchymal transition in the proximal tubular epithelial cells: contribution to oxalate kidney injury. Sci. Rep. 7, 1–12.

Dai, H., Deng, H.B., Wang, Y.H., Guo, J.J., 2018. Resveratrol inhibits the growth of gastric cancer via the wnt/β-catenin pathway. Oncol. Lett. 16, 1579–1583.

Favale, N.O., Santacreu, B.J., Pescio, L.G., Marquez, M.G., Sterin-speziale, N.B., 2015. Sphingomyelin metabolism is involved in the differentiation of MDCK cells induced by environmental hypertonicity. J. Lipid Res. 56, 786–800.

Favale, N.O., Saterin-Speziale, N.B., Fernández Tome, M.C., 2007. Hypertonic-induced lamin A/C synthesis and distribution to nucleoplasmic speckles is mediated by TonEBP/NFAT5 transcriptional activator. Biochem. Biophys. Res. Commun. 364 (3), 443–449.

Gerardi, G., Cavia-Saiz, M., del Pino-García, R., Rivero-Pérez, M.D., González-SanJosé, M.L., Muñiz, P., 2020a. Wine pomace product ameliorates hypertensive and diabetic aorta vascular remodeling through antioxidant and anti-inflammatory actions. J. Funct. Foods 66, 103794.

Gerardi, G., Cavia-Saiz, M., Rivero-Pérez, M.D., González-SanJosé, M.L., Muñiz, P., 2019. Modulation of Akt-p38-MAPK/Nrf2/SIRT1 and NF-κB pathways by wine pomace product in hyperglycemic endothelial cell line. J. Funct. Foods 58, 255–265.

Gerardi, G., Cavia-Saiz, M., Rivero-Pérez, M.D., González-SanJosé, M.L., Muñiz, P., 2020b. Wine pomace product modulates oxidative stress and microbiota in obesity high-fat diet-fed rats. J. Funct. Foods 68, 103903.

Gerardi, G., Cavia-Saiz, M., Rivero-Pérez, M.D., González-SanJosé, M.L., Muñiz, P., 2020c. The protective effects of wine pomace products on the vascular endothelial barrier function. Food Funct. 11 (9), 7878–7891.

Getting, J.E., Gregoire, J.R., Phul, A., Kasten, M.J., 2013. Oxalate nephropathy due to "juicing": case report and review. Am. J. Med. 126, 768–772.

Gray, A.L., Stephens, C.A., Bigelow, R.L.H., Coleman, D.T., Cardelli, J.A., 2014. The polyphenols (-)-Epigallocatechin-3-gallate and luteolin synergistically inhibit TGF-β-induced myofibroblast phenotypes through rhoa and ERK inhibition. PLoS One 9.

Herzlinger, D.A., Easton, T.G., Ojakian, G.K., 1982. The MDCK epithelial cell line expresses a cell surface antigen of the kidney distal tubule. J. Cell Biol. 93, 269–277.

Holthoff, J.H., Wang, Z., Seely, K.A., Gokden, N., Mayeux, P.R., 2012. Resveratrol improves renal microcirculation, protects the tubular epithelium, and prolongs survival in a mouse model of sepsis-induced acute kidney injury. Kidney Int. 81, 370–378.

Hsu, S., Bollag, W.B., Lewis, J., Huang, Q.I.N., Singh, B., Sharawy, M., Yamamoto, T., Schuster, G., 2003. Green tea polyphenols induce differentiation and proliferation in epidermal keratinocytes. J. Pharmacol. Exp. Ther. 306, 29–34.

Kalluri, R., a Weinberg, R., 2009. The basics o epithelial-mesenchymal transition. J. Clin. Invest. 119, 1420–1428.

Kanlaya, R., Khamchun, S., Kapincharanon, C., 2016. Protective effect of via Nrf2 pathway against oxalate- induced epithelial mesenchymal transition (EMT) of renal tubular cells. Nat. Publ. Gr. 1, 1–13.

Khand, F.D., Gordge, M.P., Robertson, W.G., Noronha-Dutra, A.A., Hothersall, J.S., 2002. Mitochondrial superoxide production during oxalate-mediated oxidative stress in renal epithelial cells. Free Radic. Biol. Med. 32, 1339–1350.

Kim, Y.N., Choe, S.R., Cho, K.H., Cho, D.Y., Kang, J., Park, C.G., Lee, H.Y., 2017. Resveratrol suppresses breast cancer cell invasion by inactivating a RhoA/YAP signaling axis. Exp. Mol. Med. 49, e296–e299.

Kültz, D., 2004. Hypertonicity and TonEBP promote development of the renal concentrating system. Am. J. Physiol. Ren. Physiol. 287, 876–877.

Lamouille, S., Xu, J., Derynck, R., 2014. Molecular mechanisms of epithelial–mesenchymal transition Samy. Nat. Rev. Mol. Cell Biol. 15, 178–196.

Li, S., Yan, T., Deng, R., Jiang, X., Xiong, H., Wang, Y., Yu, Q., Wang, X., Chen, C., Zhu, Y., 2017. Low dose of kaempferol suppresses the migration and invasion of triple-negative breast cancer cells by downregulating the activities of RhoA and Rac1. OncoTargets Ther. 10, 4809–4819.

Liu, Y., 2010. New insights into epithelial-mesenchymal transition in kidney fibrosis. J. Am. Soc. Nephrol. 21, 212–222.

Mohana, S., Ganesan, M., Rajendra Prasad, N., Ananthakrishnan, D., Velmurugan, D., 2018. Flavonoids modulate multidrug resistance through wnt signaling in P-glycoprotein overexpressing cell lines. BMC Canc. 18, 1–11.

Pescio, L.G., Favale, N.O., Márquez, M.G., Sterin-Speziale, N.B., 2012. Glycosphingolipid synthesis is essential for MDCK cell differentiation. Biochim. Biophys. Acta Mol. Cell Biol. Lipids 1821, 884–894.

Pescio, L.G., Santacreu, B.J., Lopez, V.G., Humberto, C., Romero, D.J., Sterin-speziale, N.B., 2017. Changes in ceramide metabolism are essential in Madin-Darby canine kidney cell differentiation. J. Lipid Res. 58, 1428–1438.

Del Pino-García, R., García-Lomillo, J., Rivero-Pérez, M.D., González-Sanjosé, M.L., Muñiz, P., 2015. Adaptation and validation of QUick, easy, new, CHEap, and reproducible (QUENCHER) antioxidant capacity assays in model products obtained from residual wine pomace. J. Agric. Food Chem. 63, 6922–6931.

Del Pino-García, R., Rivero-Pérez, M.D., González-Sanjosé, M.L., Castilla-Camina, P., Croft, K.D., Muñiz, P., 2016. Attenuation of oxidative stress in Type 1 diabetic rats supplemented with a seasoning obtained from winemaking by-products and its effect on endothelial function. Food Funct. 7, 4410–4421.

Del Pino-García, R., Rivero-Pérez, M.D., González-SanJosé, M.L., Croft, K.D., Muñiz, P., 2017. Antihypertensive and antioxidant effects of supplementation with red wine pomace in spontaneously hypertensive rats. Food Funct. 8, 2444–2454.

Rao, R., 2008. Oxidative stress-induced disruption of epithelial and endothelial tight junctions radhakrishna. Front. Biosci. 1, 7210–7226. Natural.

Rashed, T., Menon, M., Thamilselvan, S., 2004. Molecular mechanism of oxalate-induced free radical production and glutathione redox imbalance in renal epithelial cells: effect of antioxidants. Am. J. Nephrol. 24, 557–568.

Rindler, M.J., Chuman, L.M., Shaffer, L., Saier, M.H., 1979. Retention of differentiated properties in an established dog kidney epithelial cell line (MDCK). J. Cell Biol. 81, 635–648.

Santacreu, B.J., Pescio, L.G., Romero, D.J., Corradi, G.R., Sterin-Speziale, N., Favale, N.O., 2019. Sphingosine kinase and sphingosine-1-phosphate regulate epithelial cell architecture by the modulation of de novo sphingolipid synthesis. PLoS One 14, e0213917.

Sferrazza, G., Corti, M., Brusotti, G., Pierimarchi, P., Temporini, C., Serafino, A., Calleri, E., 2020. Nature-derived compounds modulating Wnt/b-catenin pathway: a preventive and therapeuticopportunity in neoplastic diseases. Acta Pharm. Sin. B.

Vargas, F., Romecín, P., García-guillén, A.I., Wangesteen, R., Vargas-tendero, P., Paredes, M.D., Atucha, N.M., Lambert, E., Morris, B.J., 2018. Flavonoids in kidney Health and disease. Front. Physiol. 9, 1–12.

Weber, K., Casali, C., Gaveglio, V., Pasquaré, S., Morel Gómez, E., Parra, L., Erjavec, L., Perazzo, C., Fernández Tome, M.C., 2018. TAG synthesis and storage under osmotic stress. A requirement for preserving membrane homeostasis in renal cells. Biochim. Biophys. Acta Mol. Cell Biol. Lipids 1863, 1108–1120.

Wei, Q., Huang, H., 2013. Insights into the role of cell-cell junctions in physiology and disease. Cell. Mol. Biol. 306, 187–221.